

AD-A154 937

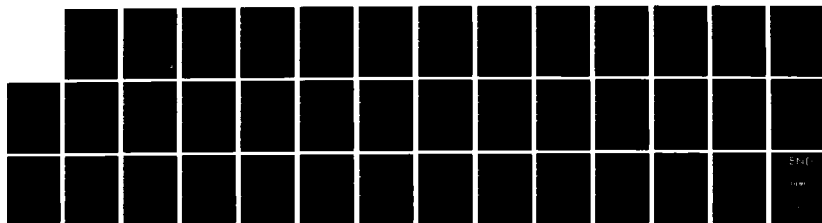
THE SPACE SHUTTLE GLOW(U) HARVARD COLL OBSERVATORY
CAMBRIDGE MA A DALGARNO 17 OCT 84 AFGL-TR-84-0281
F19628-84-K-0001

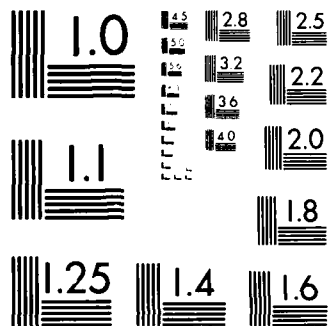
1/1

UNCLASSIFIED

F/G 22/2

NL





(2)

AD-A154 937

AFGL-TR-84-0281

THE SPACE SHUTTLE GLOW

A. Dalgarno

Harvard College Observatory
Cambridge, MA 02138

Final Report
2 November 1983 - 30 September 1984

17 October 1984

Approved for public release; distribution unlimited

DTIC FILE COPY

AIR FORCE GEOPHYSICS LABORATORY
AIR FORCE SYSTEMS COMMAND
UNITED STATES AIR FORCE
HANSCOM AFB, MASSACHUSETTS 01731

DTIC
SELECTED
JUN 12 1985
G

85 5 17 05 3

This report has been reviewed by the ESD Public Affairs Office (PA) and is releasable to the National Technical Information Services (NTIS).

"This technical report has been reviewed and is approved for publication"

Edmond Murad

EDMOND MURAD
Contract Manager

Charles P. Pike

CHARLES P. PIKE, Chief
Spacecraft Interactions Branch
Space Physics Division

FOR THE COMMANDER

Rita C. Sagalyn

RITA C. SAGALYN, Director
Space Physics Division

Qualified requestors may obtain additional copies from the Defense Technical Information Center. All others should apply to the National Technical Information Service.

If your address has changed, or if you wish to be removed from the mailing list, or if the addressee is no longer employed by your organization, please notify AFGL/DAA, Hanscom AFB, MA 01731. This will assist us in maintaining a current mailing list.

Do not return copies of this report unless contractual obligations or notices on a specific document requires that it be returned.

The following

SECURITY CLASSIFICATION OF THIS PAGE

REPORT DOCUMENTATION PAGE				
1a. REPORT SECURITY CLASSIFICATION Unclassified		1b. RESTRICTIVE MARKINGS		
2a. SECURITY CLASSIFICATION AUTHORITY		3. DISTRIBUTION/AVAILABILITY OF REPORT Approved for public release; distribution unlimited		
2b. DECLASSIFICATION/DOWNGRADING SCHEDULE				
4. PERFORMING ORGANIZATION REPORT NUMBER(S)		5. MONITORING ORGANIZATION REPORT NUMBER(S) AFGL-TR-84-0281		
6a. NAME OF PERFORMING ORGANIZATION Harvard College Observatory		6b. OFFICE SYMBOL (If applicable)		7a. NAME OF MONITORING ORGANIZATION
7b. ADDRESS (City, State and ZIP Code) Cambridge, MA 02138				
8a. NAME OF FUNDING/SPONSORING ORGANIZATION Air Force Geophysics Laboratory		8b. OFFICE SYMBOL (If applicable) PHK		9. PROCUREMENT INSTRUMENT IDENTIFICATION NUMBER F19628-84-K-0001
8c. ADDRESS (City, State and ZIP Code) Randolph AFB, MA 01731 Monterey/Edmond Murad/		10. SOURCE OF FUNDING NOS.		
		PROGRAM ELEMENT NO. 62101F	PROJECT NO. 6687	TASK NO. 11 AD
11. TITLE (Include Security Classification) THE SPACE SHUTTLE GLOW				
12. PERSONAL AUTHOR(S) A. Dalmanno				
13a. TYPE OF REPORT Final		13b. TIME COVERED FROM 11/2/83 TO 9/30/84		14. DATE OF REPORT (Yr. Mo., Day) 1984 October 17
15. PAGE COUNT 38				
16. SUPPLEMENTARY NOTATION 0				
17. COSATI CODES		18. SUBJECT TERMS (Continue on reverse if necessary and identify by block number)		
FIELD	GROUP	SUB. GR.	Shuttle glow; Radiative lifetime; AE-Glow; Day-Night variation; satellite lifetime dependence; plasma environment dependence.	
19. ABSTRACT (Continue on reverse if necessary and identify by block number) Photographic pictures of the shuttle glow were analyzed. Radiative lifetime of the emitting species was found to be 0.7 msec by analyzing the spatial distribution of the glow intensity. The AE-glow under daytime conditions has been examined. The glow was more intense in the daytime, but the production efficiency, measured in Rayleighs per oxygen atom, was found to be similar to the nighttime value. No dependence of the glow intensity on the ambient density was found. The production efficiency increased with time throughout the duration of the satellite in orbit. <i>Keywords:</i>				
20. DISTRIBUTION/AVAILABILITY OF ABSTRACT UNCLASSIFIED/UNLIMITED SAME AS RPT DTIC USERS		21. ABSTRACT SECURITY CLASSIFICATION Unclassified		
22a. NAME OF RESPONSIBLE INDIVIDUAL Edmond Murad		22b. TELEPHONE NUMBER (Include Area Code) (617) 861-3046		22c. OFFICE SYMBOL PHK

DD FORM 1473, 83 APR

EDITION OF 1 JAN 73 IS OBSOLETE.

UNCLASSIFIED
SECURITY CLASSIFICATION OF THIS PAGE

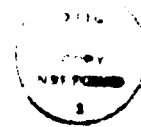
1. Introduction

The spacecraft-environment induced optical glow has attracted wide attention since the photographs from the third Space Shuttle mission indicating that the orbiter glows in the dark were released (Bank et al. 1983). The emission is a potential optical contaminant in astronomical and aeronautical experiments planned for future space shuttle missions.

A similar emission has been observed in photometric measurements on board other spacecraft (Torr et al. 1977; Yee and Abreu 1982a). By correcting for the galactic background and filtering out the airglow emission in the Visible Airglow Experiment (VAE) measured intensities on board the Atmosphere Explorer (AE) satellite, Yee and Abreu (1982b) presented a detailed study of the characteristics of the glow emission at 7320 A and 6563 A. They found that the most intense radiation comes from the surfaces facing the direction of motion of the satellite. There is a strong correlation between the emission intensity and ambient atomic oxygen density in the 160-280 km altitude range. Extending their analysis to shorter wavelengths, Yee and Abreu (1983) obtained a crude spectral variation of the glow emission and reported that the emission has a diffuse band or continuum spectrum ranging from the ultraviolet to the near infrared, peaking towards the red and probably the infrared region.

Accession For	
NTIS	<input checked="" type="checkbox"/>
DTIC	<input type="checkbox"/>
Unannounced	<input type="checkbox"/>
Justification	
By	
Distribution/	
Availability Codes	
Dist	Avail and/or
Special	

11



The processes leading to the production of the glow are not fully understood. Yee and Abreu (1982b) attributed the emission to collisions of oxygen atoms with the satellite surface in which metastable molecules are formed. The metastable molecules leave the surface and radiate, producing the spatially extended glow.

The identities of the metastable molecules are uncertain. The hydroxyl OH has been suggested as a possible candidate (Slanger, 1983; Langhoff et al., 1983). The possibility of OH being responsible for the glow and whether the glow observed on the Shuttle has the same origin as the AE glow have been our main research subject for the past year.

2. Analysis of The Glow Observed on Dynamics Explorer Satellite

Because of the VAE instrument limitation, only a crude spectrum of the glow was obtained (Yee and Abreu, 1983). The spectral variation of the glow in higher resolution is necessary to establish the OH hypothesis or to identify the excited molecules producing the glow. We have analyzed the data from the Fabry-Perot Interferometer (FPI) on board the Dynamic Explorer-B satellite (paper 1 enclosed).

The DE-B satellite is a modified version of the AE satellites, and the FPI instrument is capable of measuring the glow with a resolution of ~ 0.018 Å. Data obtained by the FPI in a spectral region centered around 7320 Å were analyzed. The spectral region investigated corresponds to the 8-3 OH Meinel band, and it is very strong in the terrestrial nightglow which peaks in a layer near the mesopause. Consequently, a comparison

of the spectra obtained at mesospheric heights with those obtained from the glow emission should provide the necessary information to show whether OH is one of the emitting metastable species producing the glow.

The results indicated that the optical glow observed by Yee and Abreu at 7320 A on the AE satellites is produced by several emission lines. The comparison of the glow spectrum with the nightglow OH spectrum provided evidence that OH might be one of the species producing the glow.

3. Radiative Lifetime Analysis of the Shuttle Glow

Besides the spectral variation of the glow, the radiative lifetime is another important parameter in determining the identities of the emitting species. If the glow is produced by the radiating molecules leaving the spacecraft surface, the radiative lifetime can be estimated from the spatial extent of the glow.

A method of inferring the radiative lifetime from the photographic pictures of the shuttle glow has been developed (paper 2 enclosed). From an analysis of the AE data, Yee and Abreu (1982b) obtained an upper limit of 10^3 cm for the product of the radiative decay time and the velocity of the emitting species. For thermal velocities, the corresponding radiative lifetime has an upper limit of 10^{-2} sec, which is consistent with the calculated lifetimes of OH Meinel band. The lifetime obtained by analyzing the shuttle glow pictures can determine whether the same excited molecules are responsible for the

Shuttle glow.

By examining the extent of the glow from the photographs, we have obtained a characteristic decay length of 20 cm for the Shuttle glow, equivalent to a radiative lifetime probably lying between 0.3 and 1.3 msec. This is much shorter than the OH Meinel band radiative lifetimes, suggesting that some other excited species besides OH is producing the Shuttle glow.

The intensity of Shuttle glow is also estimated by comparing it with the airglow feature seen at the limb of the earth in the picture. We find that the maximum glow intensity is about three times more intense than the airglow, giving for the Shuttle glow an estimated intensity of about 750 kR and a production efficiency of 2.5×10^{-6} photons per one atomic oxygen impact in the visible range of the spectrum.

4. Mechanism Leading to the Production of the Excited molecules

The processes leading to the production of the glow are not fully understood. We have suggested that metastable molecules are created by the impact of atmospheric oxygen atoms with the spacecraft surface through either direct impact excitation or surface chemical reactions. An alternative theory has been proposed by Papadopoulos (1984) who suggests that plasma interactions produce suprathermal electrons and ions which excite the ambient gaseous and surface materials. Thus, the magnitude of the ambient plasma density controls the intensity of the glow intensity. We therefore extend our AE data analysis to daytime observation of the glow and compare the intensities observed

during periods of solar minimum and solar maximum when the ambient plasma densities were relatively larger (paper 3 enclosed).

Our study indicated that the ratio of the glow intensity and the ambient atomic oxygen density increased through the lifetime of the satellite which covered the increasing phase of the solar cycle. The increase of $I/n(O)$ with time appears not to be a consequence of the enhancement of ambient plasma activity. No significant increase of glow intensity was found as the satellite moved from nighttime to daytime although the plasma density increased by almost one order of magnitude. The increase of $I/n(O)$ with satellite lifetime indicates that collisions with the atmosphere caused modifications in the satellite surface.

The plasma theory of Papadopoulos is not consistent with the characteristics of the glow observed on the AE satellite. However, the AE satellite may be too small in size to initiate a plasma controlled glow phenomenon and our conclusions may not apply to the glow observed on the Shuttle.

5. Summary

Our research on the spacecraft-environment induced glow for the past year can be summarized as follows:

1. The OH Meinel band seems to be a plausible candidate for the AE and DE satellite glow.
2. The radiative lifetime of the emitting species deduced from the Shuttle glow is shorter than that of the OH Meinel band, indicating that OH may be excluded as the species responsible

for the Shuttle glow at least in the visible region of the spectrum.

3. The plasma alternative model suggested for the Shuttle glow cannot explain the characteristics of the AE glow.
4. The AE glow production efficiency increased through the satellite lifetime, indicating a possible modification of the satellite surface.

ENCLOSURES

1. Abreu, V.J., W.R. Skinner, P.B. Hays and J.H. Yee,
"Optical Effects of Spacecraft-Environment Interaction:
Spectrometric Observations by the DE-B Satellite", Proceedings of
AIAA Shuttle Environment and Operations Meeting, 1983 and Journal
of Spacecraft and Rockets, 1984 in press.
2. Yee, J.H. and A. Dalgarno, "Radiative Lifetime Analysis of the
Shuttle Optical Glow", Proceedings of AIAA Shuttle Environment and
Operations Meeting, 1983, and submitted to Journal of Spacecraft
and Rockets, 1984.
3. Yee, J.H. and A. Dalgarno, "Characteristics of the Spacecraft
Optical Glow", Geophysical Research Letters, 1984, in press.

REFERENCES

1. Banks, P.M., P.R. Williamson, and W.J. Raitt, "Space Shuttle
glow Observations", Geophys. Res. Lett. 10, 118, 1983.
2. Langhoff, S.R., R.L. Jaffe, J.H. Yee, and A. Dalgarno, "The
surface Glow of the Atmosphere Explorer C and E Satellites",
Geophys. Res. Lett., 10, 896, 1983.
3. Papadopoulos, D., "On the Shuttle Glow (The Plasma Alternative)",
Radio Sci., 19, 571, 1984.
4. Slanger, T.G., "Conjectures on the origin of the surface glow
of space vehicles", Geophys. Res. Lett., 10, 130, 1983.
5. Torr, M.R., P.B. Hays, B.C. Kennedy and J.C.G. Walker,
"Intercalibration of airglow observations with the Atmosphere
Explorer Satellites", Planet. Space Sci., 25, 173, 1977.
6. Yee, J.H. and V.J. Abreu, "Exospheric temperatures deduced from
7320-7330 Å ($O^+(2p)-C^+(2D)$) twilight observations, J. Geophys.
Res., 87, 193, 1982a.

7. Yee, J.H. and V.J. Abreu, "Optical contamination on the Atmosphere Explorer-E satellite", Proceedings of SPIE Technical Symposium, 338, 120, 1982b.

8. Yee, J.H. and V.J. Abreu, "Visible Glow Induced by Spacecraft-environment interaction", Geophys. Res. Lett., 10, 126, 1983.

CHARACTERISTICS OF THE SPACECRAFT OPTICAL GLOW

Jeng-Hwa Yee, V. J. Abreu^{*} and A. Dalgarno

Harvard-Smithsonian Center for Astrophysics
60 Garden Street, Cambridge, Massachusetts 02138

^{*}Space Physics Research Laboratory
University of Michigan, Ann Arbor, Michigan 48109

ABSTRACT

The optical glow induced by spacecraft-environment interaction under daytime conditions is analyzed using photometric data obtained by the Visible Airglow Experiment on board the Atmosphere Explorer Satellite. Because of the increased ambient oxygen density, the glow is more intense in the daytime. The daytime production efficiency, measured in Rayleighs per oxygen atom, is similar to the nighttime value. No dependence of the glow intensity on the ambient plasma density was found. The production efficiency increased with time throughout the duration of the spacecraft in orbit.

AIAA-83-2660

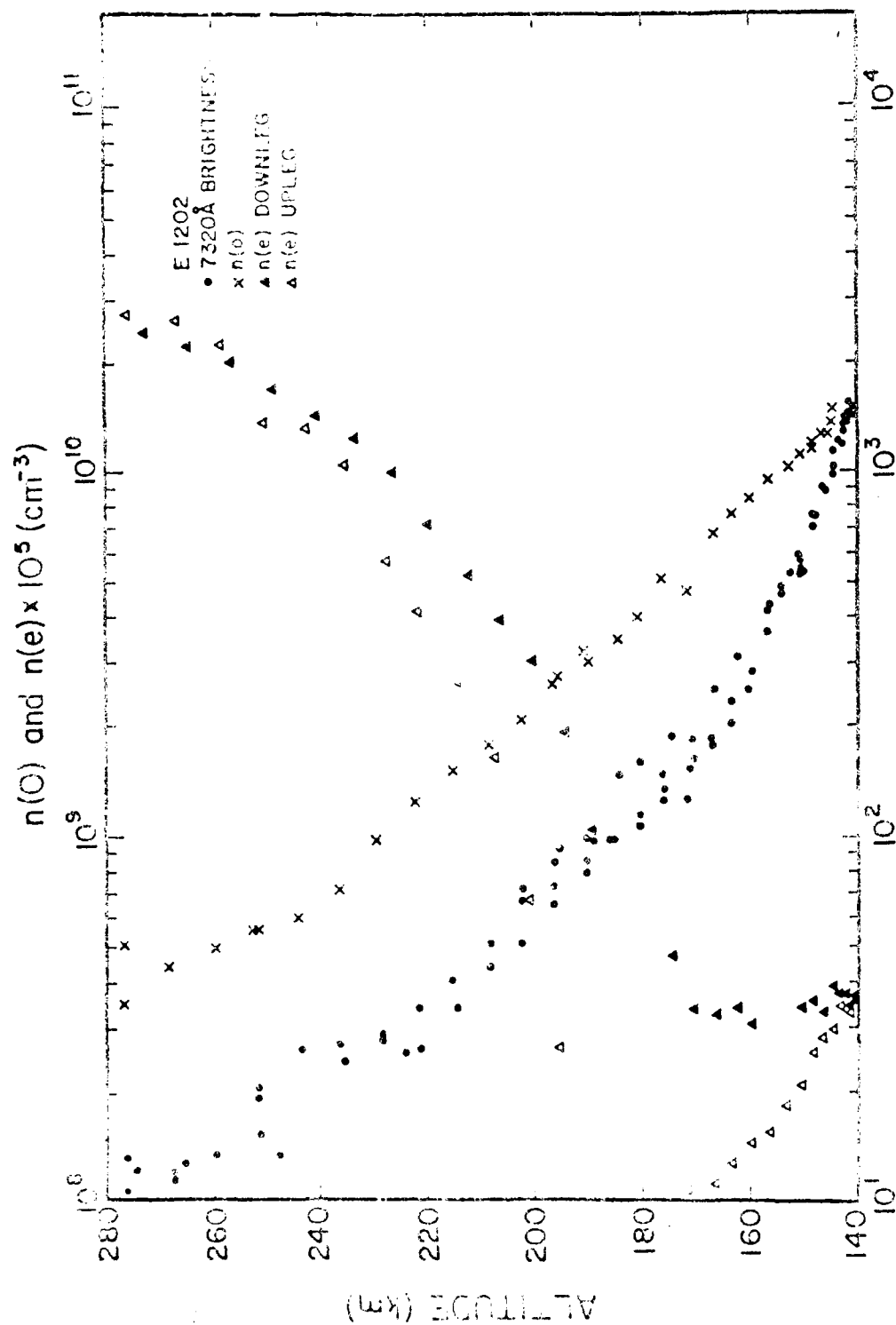
**Radiative Lifetime Analysis of the Shuttle Optical
Glow**

J.H. YEE and A. DALGARNO

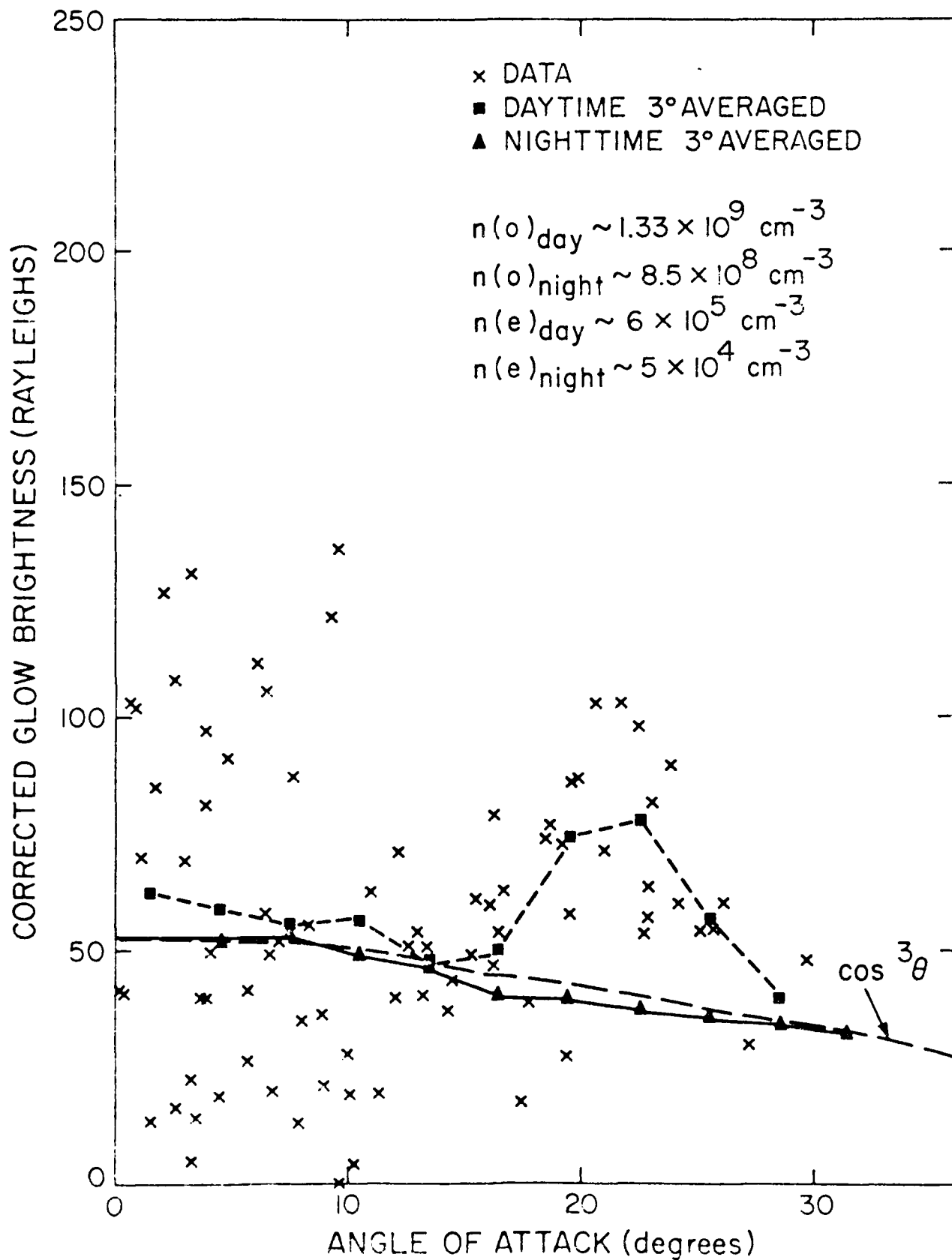
**AIAA SHUTTLE ENVIRONMENT
AND OPERATIONS MEETING**

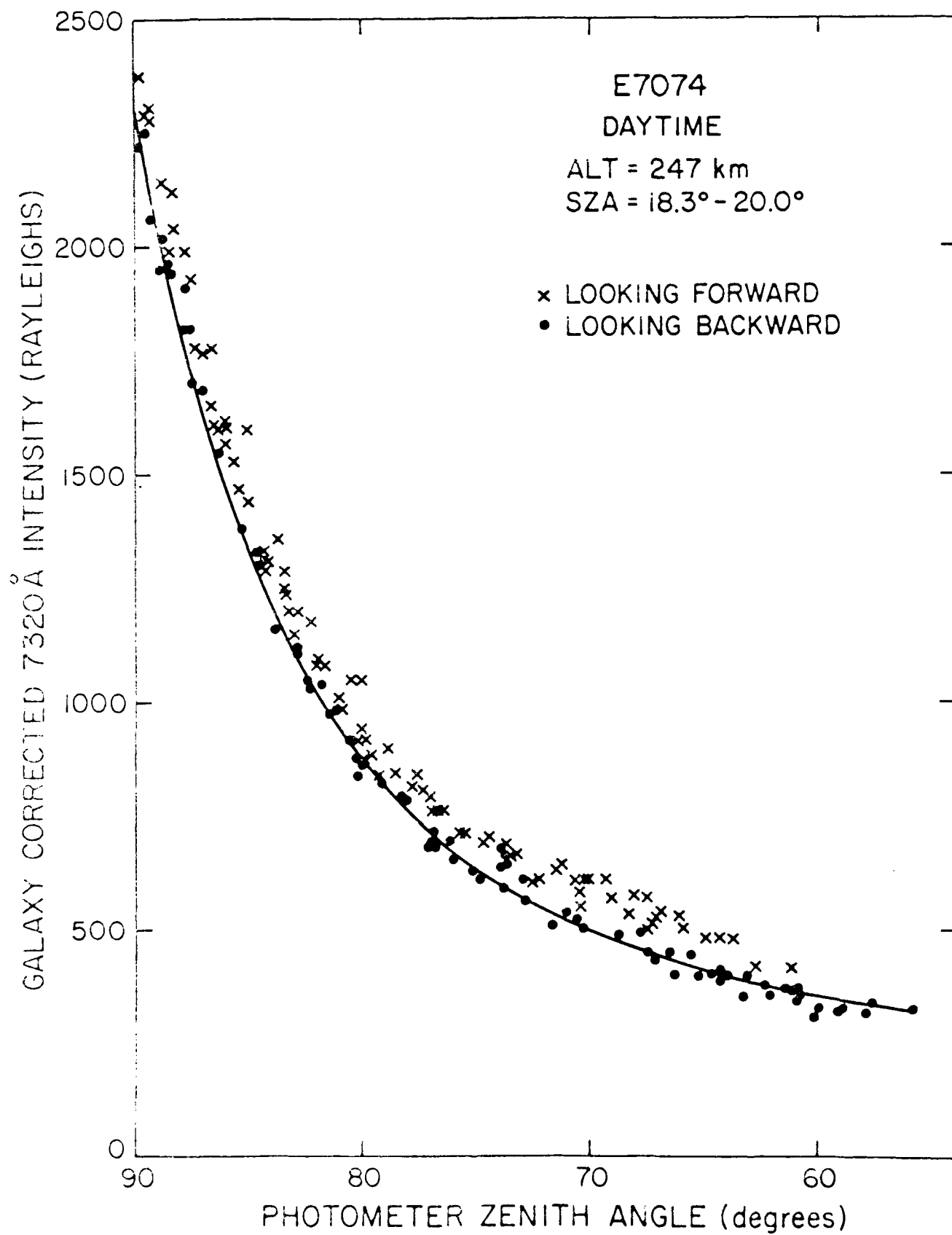
OCTOBER 31 - NOVEMBER 2, 1983 WASHINGTON, DC

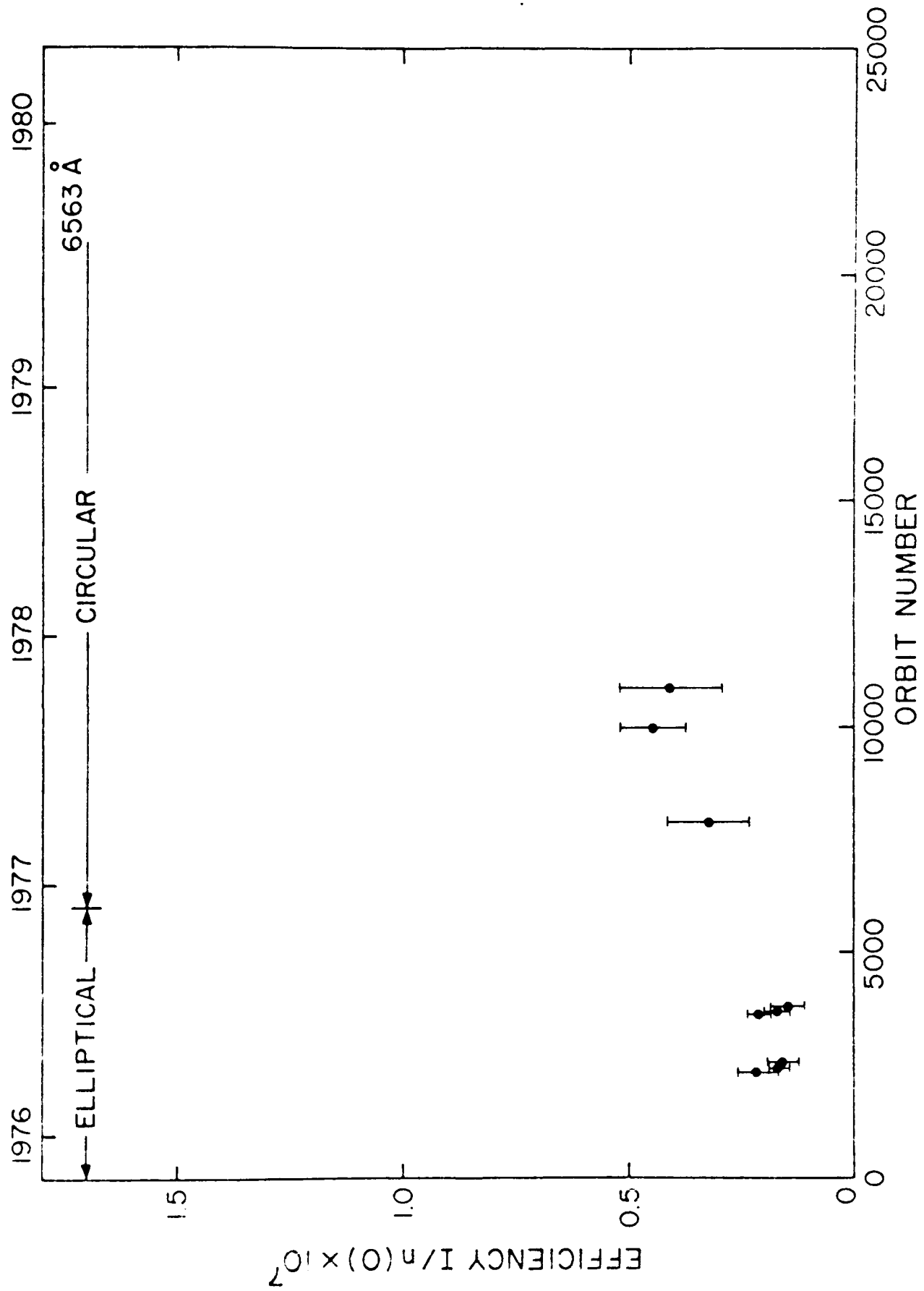
Published by the American Institute of Aeronautics and Astronautics, 1801 Alexander Bell Drive, Suite 400, Alexandria, Virginia 22304



7320Å BRIGHTNESS (RAYLEIGHS)







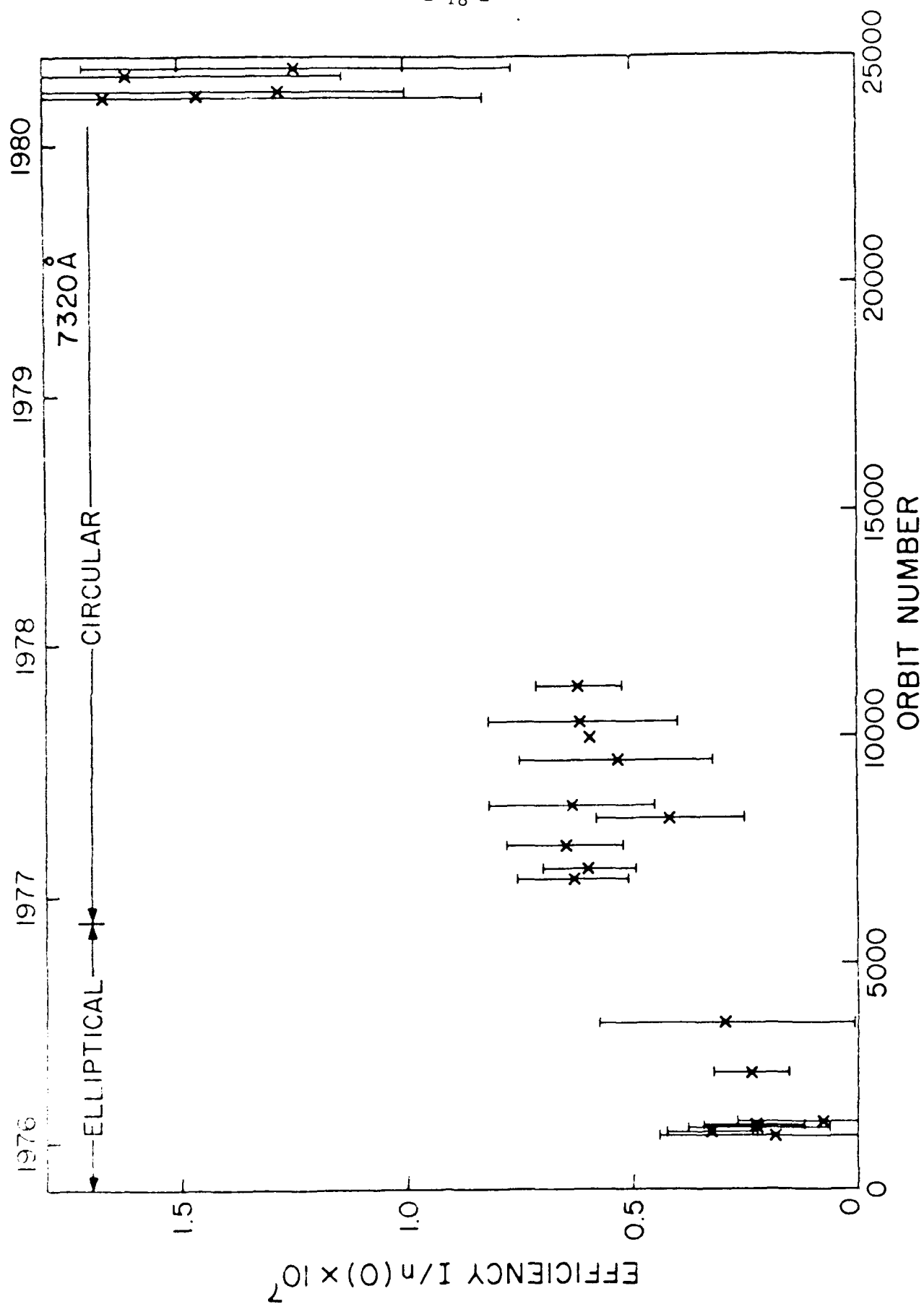


FIGURE CAPTIONS

Figure 1: Observed $I/n(O)$ at 7320 Å (a) and 6563 Å (b) as a function of time or orbit number.

Figure 2: (a) Background corrected results of 7320 Å intensity as a function photometer zenith angle.

(b) Optical glow brightness as a function of angle of attack.

Figure 3: Altitude profile of the glow intensity versus the ambient atomic oxygen and electron densities.

REFERENCES

- Abreu, V.J., J.H. Yee and P.B. Hays, "Galactic and Zodiacal light surface brightness measurements with the Atmosphere Explorer Satellites", App. Opt. 21, 2287, 1982.
- Banks, P.M., P.R. Williamson, and W.J. Raitt, "Space Shuttle glow Observations", Geophys. Res. Lett. 10, 118, 1983.
- Hays, P.B., G. Carignan, B.C. Kennedy, G.G. Shepherd and J.C.G. Walker, "The Visible-Airglow Experiment on Atmosphere Explorer", Radio Sci. 8, 369, 1973.
- Papadopoulos, K., "On the Shuttle Glow (The plasma alternative)", Radio Science, 19, 571, 1984.
- Torr, M.R., P.B. Hays, B.C. Kennedy, and J.C.G. Walker, "Inter-calibration of airglow observations with the Atmosphere Explorer Satellites", Planet. Space Sci. 25, 173, 1977.
- Yee, J.H. and V.J. Abreu, "Exospheric temperatures deduced from 7320-7330 Å ($O^+(^2P-O^+(^2D))$) twilight observations", J. Geophys. Res. 87, 193, 1982a.
- Yee, J.H. and V.J. Abreu, "Optical contamination on the Atmosphere Explorer-E satellite, "Proceedings of SPIE Technical Symposium, 338, 120, 1982b.
- Yee, J.H. and V.J. Abreu, "Visible Glow induced by spacecraft-environment interaction", Geophys. Res. Lett. 10, 126, 1983.

The plasma theory (Papadopoulos 1984) is not consistent with the characteristics of the glow observed on the AE satellite. However, the AE satellite may be too small in size to initiate a plasma controlled glow phenomenon and our conclusions may not apply to the glow observed on the Shuttle.

ACKNOWLEDGMENTS:

This research was supported by the Aeronomy program, Division of Atmospheric Science, National Science Foundation ATM-80-25627 and by the Air Force Geophysics Laboratory under Contract F19628-84-K-0001.

leights of glow emission from hundreds or thousands of Rayleighs of airglow emission, the statistical variances in the results are large. The atomic oxygen density in the daytime averaged over the time of observation was about a factor of 1.56 larger than the night-time density. The ambient electron density in the daytime was about one order of magnitude larger than the night-time density. The small increase of glow intensity in the daytime may be plausibly attributed to the enhanced atomic oxygen density and is apparently unrelated to the ambient plasma density.

2.3 Glow Intensity Altitude Profile:

Figure 3 gives the altitude profile of the glow intensity at 7320 \AA along with the measured number densities of atomic oxygen and electrons. It shows that above 160 km, the glow intensity is governed by the atomic oxygen density and is not affected by the activity of the ambient plasma environment.

III. CONCLUSION

We have found that the ratio of the glow intensity and the ambient atomic oxygen density increased through the lifetime of the satellite which covered the increasing phase of the solar cycle. The increase of $I/n(O)$ with time appears not to be a consequence of the enhancement of ambient plasma activity. No significant increase of glow intensity was found as the satellite moved from night-time to daytime although the plasma density increased by almost one order of magnitude. The increase of $I/n(O)$ with satellite lifetime indicates that collisions with the atmosphere caused sputterings in the satellite surface.

period. All the data obtained earlier (Yee and Abreu 1982a,b) referred to night-time orbits for which a special technique was used to separate the galactic background brightness from the glow brightness. The existence of dayglow emission as well as the brighter zodiacal light makes the analysis of the spacecraft-environment induced glow in the daytime more difficult.

In analyzing the daytime data, we first subtracted the galactic background brightness obtained from the zodiacal light and diffuse star brightness maps generated by Abreu et al. (1982). Figure 2a gives the corrected results for circular orbit 7074 for a satellite solar zenith angle between 18.3° and 20.0° and plots them as a function of photometer zenith angle. The crosses represent the forward-looking data obtained when the photometer was looking into the ram direction and the dots represent the backward-looking data. Because the zodiacal light is intense within 60° of the sun, data with zenith angles less than 60° are not useful.

The backward-looking data contain only the airglow emission and are free of any interaction-induced glow (Yee and Abreu, 1982a,b). If we assume that the airglow brightness is symmetric around the photometer zenith (which should be the case at solar zenith minimum), the glow intensity can be obtained by subtracting the backward-looking data from the forward-looking data.

The results, averaged over every 3° , are plotted in Figure 2b. The night-time data are shown for comparison. It is clear that the glow intensity in the daytime is larger than in the nighttime. Because we are trying to separate tens of Ray-

provides an opportunity to examine the variation of the glow intensity with solar activity.

Yee and Abreu (1982b) analyzed 12 orbits of night-time VAE data at 7320 \AA taken during the first two years of the AE-E mission. They reported that the ratio between the observed glow intensity and ambient atomic oxygen density increased by a factor of 2 during the two years of low solar activity and attributed the increase to the difference in orbital type, elliptical or circular orbits. Yee and Abreu (1982a) had reported the existence of the glow during solar maximum periods while the satellite was at altitudes near 430 km. Figure 1a shows the observed ratio of the intensity I at 7320 \AA and the number density of atomic oxygen $N(O)$ as a function of time or orbit number. It shows that regardless of satellite orbital type, $I/n(O)$ increases with time along with the increase in solar activity.

Figure 1b presents the results for 6563 \AA . Because of the lack of data beyond orbit number 11000, no information under high solar activity conditions was obtained. The 6563 \AA data show similar behavior to the 7320 \AA data in that $I/n(O)$ increases with time.

2.2 Night-time and Daytime Variation:

The low inclination of the AE-E satellite permitted the acquisition of a complete diurnal set of data in an orbital

a diffuse band or continuum spectrum ranging from the ultraviolet to the near infrared, peaking towards the red and probably the infrared region.

The processes leading to the production of the glow are not fully understood. Yee and Abreu (1982b) suggested that the glow is created by the collision of oxygen atoms with the satellite surface on which metastable molecular species are formed. The metastable molecules leave the surface and radiate, producing the spatially extended glow.

An alternative theory has been proposed by Papadopoulos (1984) who suggests that plasma interactions produce suprathermal electrons and ions which excite the ambient gaseous and surface materials.

In the present study we extend the analysis to daytime observations of the glow. We compare the intensities observed during periods of solar minimum and solar maximum and we determine the changes in the glow intensities as the satellite moves from night-time to daytime. We demonstrate that the glow intensity is not correlated with the ambient electron density.

2. AE-SATELLITE GLOW

2.1 Solar Activity Variation:

The AE satellite was a self-fueled spacecraft and the on-board propulsion system allowed the satellite to remain in orbit for several years. The AE-E satellite was launched in late 1975 and re-entered in 1980. The lifetime of its mission covered the increasing phase of the present solar cycle 21 and

I. INTRODUCTION

The spacecraft-environment induced optical glow has brought wide attention since the photographs from the third Space Shuttle mission indicating that the orbiter glows in the dark were released (Banks et al. 1982). The emission is a potential optical contaminant in astronomical and aeronautical experiments planned for future space shuttle missions.

A similar emission has been observed in photometric measurements on board other spacecraft. Torr et al. (1977) noticed some enhancements in the airglow intensities below 170 km measured by the Visible Airglow Experiment (VAE) on board the Atmosphere Explorer-C satellite (Hays et al. 1973) which they attributed to some form of interaction between satellite and the ambient atmosphere. Yee and Abreu (1982a) later reported observation of the glow at 7320 Å at altitudes greater than 400 km during solar maximum conditions.

By correcting for the galactic background and filtering out the airglow emission in the VAE measured intensities, Yee and Abreu (1982b) presented a detailed study of the characteristics of the glow emission at 7320 Å and 6563 Å. They found that the most intense radiation comes from the surfaces facing the direction of motion of the satellite. There is a strong correlation between the emission intensity and ambient atomic oxygen density in the 160-240 km altitude range. Extending their analysis to shorter wavelengths, Yee and Abreu (1983) obtained a crude spectral variation of the glow emission and reported that the emission has

83-2660

RADIATIVE LIFETIME ANALYSIS OF THE SHUTTLE OPTICAL GLOW

J.H. Yee and A. Dalgarno

Harvard-Smithsonian Center of Astrophysics
60 Garden Street, Cambridge, Massachusetts 02138

ABSTRACT

Photographic pictures taken during the first flight of the space shuttle revealed the presence of a diffuse optical glow above the surfaces of the vehicle in the ram direction. The origin of the glow is unknown but clearly a manifestation of the interaction of the spacecraft with the ambient atmosphere. The line of light intensity is found to be approximately three orders of magnitude more intense than the 5577 Å airglow seen at the limb of the earth. By analyzing the spatial distribution of the glow, we obtain a characteristic decay length of 10 cm. If we assume a mean orbital velocity of 3×10^4 cm sec⁻¹, the corresponding radiative lifetime is 0.67 nsec. The species responsible for the shuttle glow and the Atmosphere Explorer satellite glow appear to be different.

1. INTRODUCTION

Nighttime photographs taken by the crew of the STS-3 mission revealed that there is an optical emission of unknown origin appearing above parts of Orbiter surfaces in the ram direction of the vehicle (Figure 1). The emission has an intensity which is comparable to that of 5577 Å airglow emission seen at the limb of the earth and may be an optical contaminant to the highly sensitive astrophysical and aeronomical experiments planned for future space shuttle missions.

A similar emission has been observed in photometric measurements on board other spacecraft.¹⁻⁴ Torr et al.² noticed unexplained enhancements in the airglow intensities measured by the Visible Airglow Experiment (VAE) on board the Atmosphere Explorer-C satellite³ which they attributed to some form of interaction between the satellite and the atmosphere. After correcting the VAE measurements for the galactic background and other spectral emissions, Yee and Apert^{4,5} confirmed the finding of Torr et al.² and concluded that the intensity of the enhancement or glow is proportional to the area of the oxygen atoms with which the satellite surface on which reticulate structures and protrusions are located. The authors also suggested that the satellite and its glow, resembling the spatially extended aurora,

may be the first of the reticulate pattern of the aurora. It is not clear, however, whether the glow is a true atmospheric phenomenon or a contamination of the satellite surface. The authors also suggested that the glow may be a contamination of the satellite surface.

presented at the American Astronomical Society meeting, 1983, and published in the *Journal of Geophysical Research*, 1983.

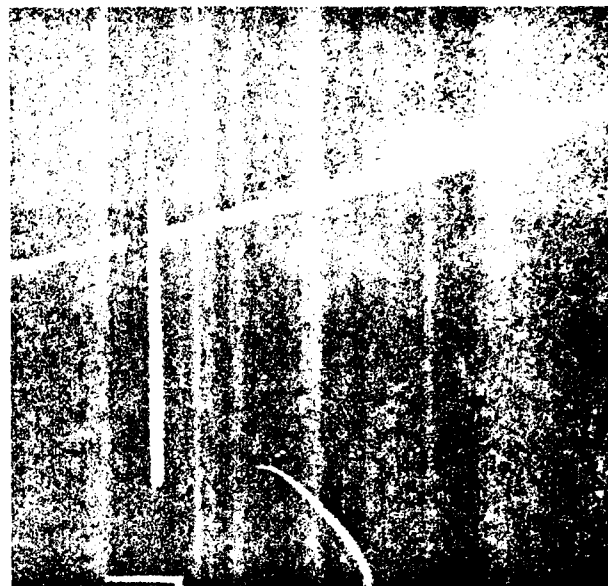


Fig. 1 Nighttime photograph of the STS-3 payload bay. The 5577 Å airglow emissions from the 100 km level of the Earth's atmosphere are visible in the background. Vehicle glow is seen above the surfaces of the vertical stabilizer and the engine pod.

red or in the infrared. Slanger⁷ pointed out that the OH airglow emissions in the spectral regions around 7320 Å and 6563 Å have the same relative intensity as the AE glow and argued that OH is a plausible candidate for the emitter. A more extensive comparison by Langhoff et al.⁸ which used spectral data over a wider range of wavelengths and which is based on an alternative model of the excitation mechanism provided support for the OH identification.

The radiative lifetime of the emitting species can be inferred from the spatial distribution of the glow intensity. From an analysis of the AE data, Yee and Apert⁴ obtained an upper limit of 1 cm for the product of the radiative decay time and the velocity of the emitting species. Assuming a velocity of 3 × 10⁴ cm sec⁻¹, the upper limit for the lifetime is an upper limit of 0.67 nsec, consistent with the calculated lifetimes of 0.4 nsec for the vibrational levels contributing to the AE glow and 0.4 nsec.

The shuttle glow has a diffuse character with a wavelength range between 4000 and 6000 Å which is similar to the AE glow spectral variation.

whether or not the above excitation rules are reasonable for the particular PLAE glow picture under consideration. In this case we must make an attempt to determine the validity of the excitation rules by comparing the results from the calculations with the glow picture of the Shuttle. We will now estimate the accuracy of the Shuttle glow picture by an estimation of the accuracy of the calculations.

II. RADIATIVE LIFETIME ANALYSIS TECHNIQUE

Consider the excited molecules with a radiative lifetime τ located in the spacecraft surface with radius R . The number density of the molecules at point P' is $n(P', \vec{V})$ in a coordinate system is shown in Fig. 2.

$$n(x, y, z) = \int \int \int n(P', \vec{V}) f(P', \vec{V}) dV d\Omega dP'$$

where $f(P', \vec{V})$ is the distribution function of the excited molecules in a spherical coordinate system with origin at P' .

According to Liouville's Theorem, the distribution function $f(P', \vec{V})$ outside the spacecraft is equal to the distribution function $f(P, \vec{V})$ at the surface by

$$f(P', \vec{V}) = f(P, \vec{V}) \exp(-\frac{R}{\tau}),$$

to include the effects of radiative decay the equation is modified, taking the form

$$f(P', \vec{V}) = f(P, \vec{V}) \exp(-\frac{R}{\tau} - \frac{R^2}{2\tau^2}),$$

where R is the distance between P' and the surface point P , provided that the velocity vector is little changing from P to P' . The number density at point P' can then be calculated from

$$n(x, y, z) = \int \int \int n(P, \vec{V}) \exp(-\frac{R}{\tau} - \frac{R^2}{2\tau^2}) dV d\Omega dP.$$

After transformation from the spherical coordinate system to the Cartesian coordinate system, we obtain

$$n(x, y, z) = \int \int \int n(P, \vec{V}) \exp(-\frac{R}{\tau} - \frac{R^2}{2\tau^2}) dV d\Omega dP.$$

After dividing the spacecraft surface element dA into a small element dA of the surface, the number density $n(P, \vec{V})$ at the surface can be calculated from the glow picture. The number density $n(P, \vec{V})$ at the surface can be calculated from the glow picture. The number density $n(P, \vec{V})$ at the surface can be calculated from the glow picture.

The number density $n(P, \vec{V})$ at the surface can be calculated from the glow picture. The number density $n(P, \vec{V})$ at the surface can be calculated from the glow picture. The number density $n(P, \vec{V})$ at the surface can be calculated from the glow picture.

The number density $n(P, \vec{V})$ at the surface can be calculated from the glow picture. The number density $n(P, \vec{V})$ at the surface can be calculated from the glow picture. The number density $n(P, \vec{V})$ at the surface can be calculated from the glow picture.

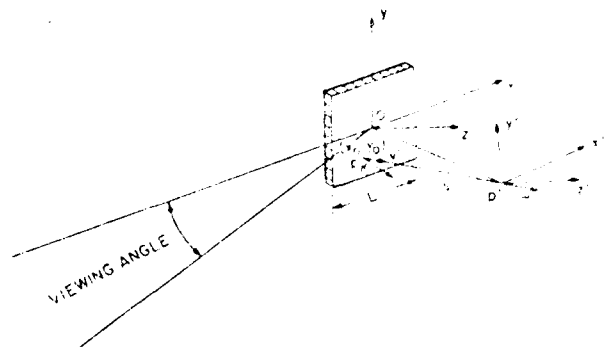


Fig. 2 Geometry used to calculate the spatial distribution of the excited molecules responsible for the glow.

inverse of the lifetime. It varies with the orientation of the spacecraft surface to the streaming ambient atmospheric particles^{1,4}. Hence the source distribution $f(P, \vec{V})$ at the surface may not be a spatially uniform function and in performing the integrations the dependence of the angle of incidence must be considered.

For a flat spacecraft surface, however, the angles between the surface normal and the velocity vector are the same everywhere at the surface, giving rise to a spatially uniform source function $f(P, \vec{V})$. From the Shuttle glow picture of figure 1, it appears that the right side of the stabilizer was facing the streaming ambient particles when the picture was taken and a flat surface can be adopted for our analysis.

EXAMPLE FOR A SPACECRAFT SURFACE WITH A SQUARE CROSS SECTION

Before analyzing the Shuttle glow picture, we consider as an example a spacecraft surface of square cross section of dimension L . The number density of the excited molecules at point P' is calculated in this case from

$$n(x, y, z) = \int \int \int n(P, \vec{V}) \exp(-\frac{R}{\tau} - \frac{R^2}{2\tau^2}) dV d\Omega dP.$$

where $R = \sqrt{(x-x_0)^2 + (y-y_0)^2 + (z-z_0)^2}$ and $P = (x_0, y_0, z_0)$.

Figure 3 presents the curves of constant ratio indicating the number density spatial distribution at $y = 0$. The characteristic length is taken to be $L = 10$ meters and the surface is a plane. The number density is obtained with the help of a computer at the center, $x = 0$, $z = 0$, and at a point (x, y, z) on the surface. The number density is obtained by the

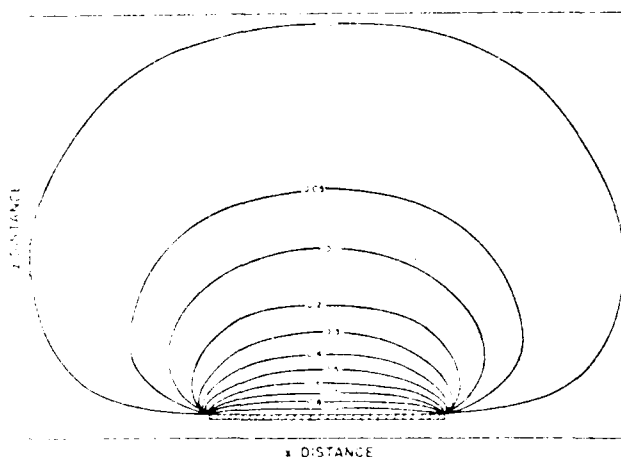


Fig. 3 Curves of constant number density above the surface of a square cross section.

solid angle subtended by the surface, modified by the radiative lifetime τ . On the z axis where $x = 0$ and $y = 0$, if the characteristic decay length is long compared to the dimension of the spacecraft ($\lambda \gg L$), the number density is controlled by the solid angle term and decreases like $1/z^2$. If $\lambda \ll L$, the number density decreases with z with an e-folding distance close to the characteristic decay length.

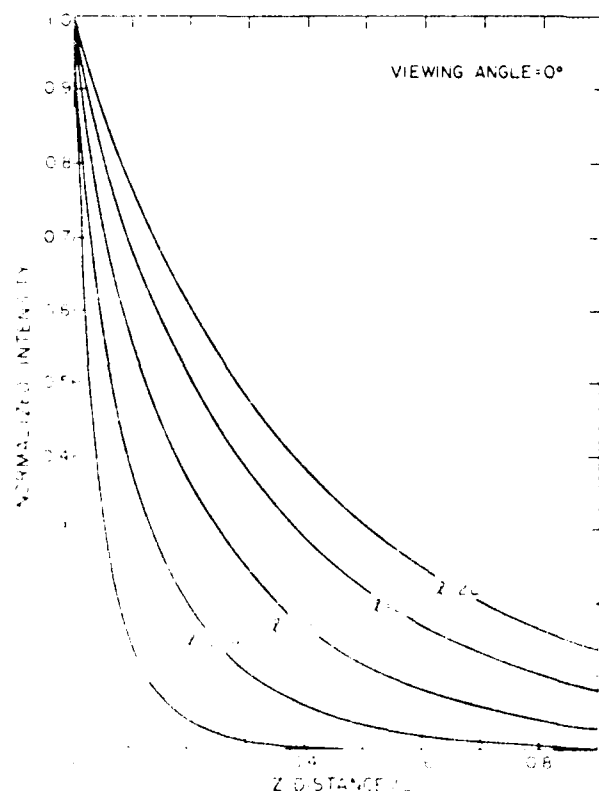


Fig. 4 Calculated line of sight glow intensity spatial distribution viewed from $\theta = 0^\circ$ for various choices of λ/L .

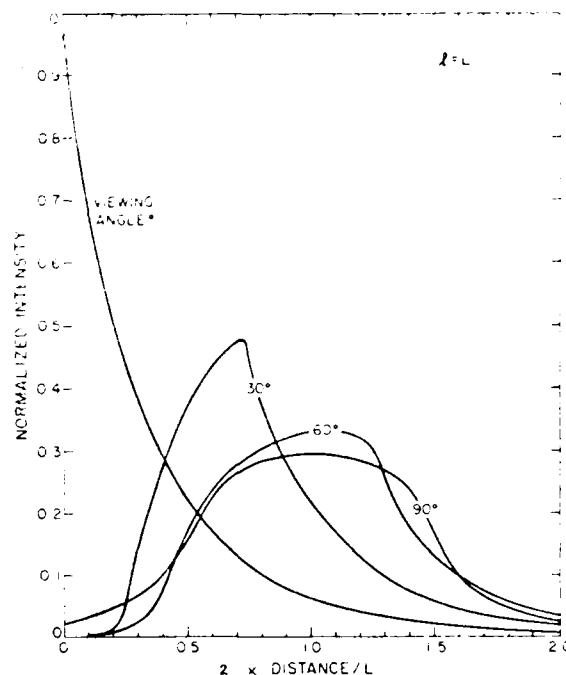


Fig. 5 Calculated line of sight intensity spatial distribution for different viewing angles.

Figure 4 shows the calculated line of sight intensities for various choices of λ as viewed along the x -axis. By comparing the calculated spatial variation with the one observed, we can infer the characteristic decay length of the excited molecules. The results we have presented are all given on a relative scale. The absolute e-folding distance deduced from the shape of the observed spatial distribution gives rise to different characteristic decay lengths for different sizes of the spacecraft surface.

The spatial distribution of the intensity is predicted to depend strongly on viewing direction. Figure 5 shows the calculated results at four different viewing angles for the case of $\lambda = L$. The maximum line of sight intensity decreases as the viewing angle increases and the glow appears to extend to a farther distance as if a longer radiative lifetime were involved. Consequently, in analyzing any measured spatial distribution of the glow intensity to infer the magnitude of λ , the viewing direction as well as the size and the shape of the spacecraft must be considered.

III. SHUTTLE STABILIZER GLOW ANALYSIS

Figure 6 gives another picture of the glow obtained during the same mission. All the photographs were taken from the aft flight deck observation window using a bracket-mounted 35mm Hasselblad camera. The pictures we present here were originally in

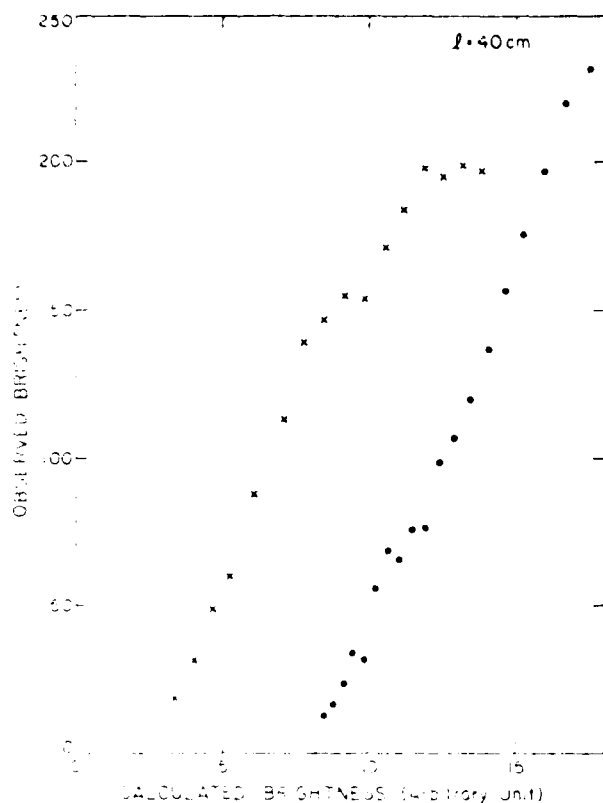


Fig. 9 The relationship between the digitized and the model calculated intensities for $l = 40$ cm.

and decreases to the noise level at approximately 45 cm with an e-folding distance of 12 cm. By comparing with the theoretically calculated spatial variations, we are able in principle to infer the characteristic decay length of the excited molecules when they leave the surface. Complications arise because the digitized intensity is not the real glow intensity. The luminosity sensitivity of the SO-489 film, the film processing and developing techniques, and system gain adjustments of the imaging procedure cause a non-linear correspondence between the digitized intensity and the actual glow intensity. An alternative approach may be more useful.

Figure 9 plots the observed intensities against the model values for a characteristic decay length l of 40 cm. The data represent the observations viewed at a distance greater than 20 cm and the circles represent those at distances less than 20 cm. Theoretically, the dots and crosses should lie on the same curve no matter what the processing procedures are. It is clear from Fig. 9 that the choice of 40 cm as the characteristic decay length is not correct.

As demonstrated in Figure 10, we found that the best agreement is obtained when the characteristic decay length is chosen to be 20 cm. In this case the observed and the calculated intensities have a linear relationship except in very intense and low exposure regions. The relationship is very similar to the granular density and log-exposure curves of the Kodak SO-489 film (Figure 11, courtesy of Kodak) used in this photograph. The film developing techniques and the system gain adjustment during the imaging processes may have distorted this characteristic curve from the one we obtained. If we assume that the excited molecules are in thermal equilibrium with the Shuttle surface and leaving it with a speed of 300 m sec^{-1} , a characteristic decay length of 20 cm gives a time constant for radiative decay of 0.67 msec.

IV. DISCUSSIONS AND CONCLUSIONS

Recent photometric and photographic observations have revealed the presence of induced optical emissions over the surface of the spacecraft due to the interaction of the spacecraft and the ambient atmosphere. It is believed that radiative emission from some unknown excited molecules formed on the spacecraft surface are responsible for the observed luminosity. In this paper we present a method to infer the radiative lifetime of the excited molecules by

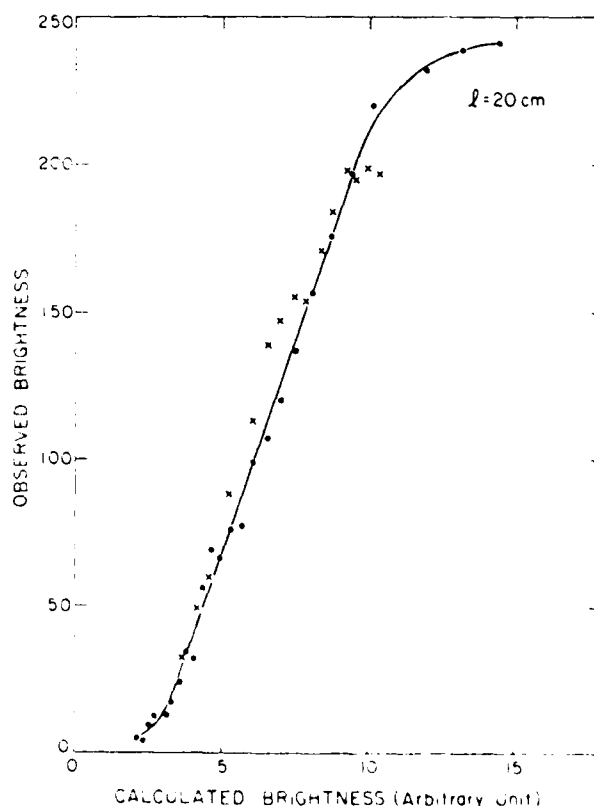


Fig. 10 The same as Figure 9 except for $l = 20$ cm.

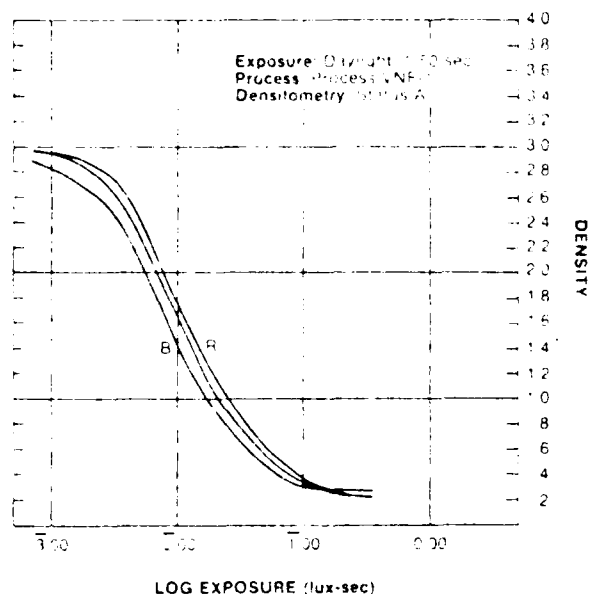


Fig. 11 The characteristic log-exposure curves for Kodak SO-489 film.

analyzing the spatial distribution of the observed intensity. We demonstrate that the observed intensity spatial distribution depends upon the shape and size of the spacecraft surface, the spacecraft orientation, and most important of all, the radiative decay length of the excited molecules.

By examining the extent of the glow from the photographs, we obtain a characteristic decay length of 20 cm for the Shuttle glow, equivalent to a radiative lifetime of approximately 0.67 msec if we assume the excited molecules are in thermal equilibrium with the surface. The radiative lifetime is an important parameter in determining the identities of the emitting excited molecules and their formation processes. The photometric data analysis suggested that the OH Meinel band system is responsible for the glow observed on the AE satellites,³ and a high resolution spectrum obtained by the Fabry-Perot Interferometer on board the Dynamic Explorer (DE) B satellite substantiates the OH hypothesis.⁴ The radiative lifetime of 0.7 msec obtained from the Shuttle glow picture is almost one order of magnitude shorter than the 10⁻⁶ sec radiative lifetime^{5,6}, suggesting that some other excitation mechanism OH is producing the Shuttle glow. An examination of the possible mechanisms is in progress.

The intensity of the Shuttle glow can be estimated by comparing it with the 5577 Å airglow measured at the limb of the earth. The intensity of the airglow at the limb is approximately 10 kR, and the Shuttle glow

intensity is approximately three times more intense than the 5577 Å airglow, giving for the Shuttle glow an estimate of 30 kR if we assume the 5577 Å airglow limb intensity is on the order of 10 kR¹. From our theoretical calculation a line of sight column intensity of 30 kR corresponds to a maximum volume emission rate of 7×10^6 photons cm⁻³sec⁻¹ or a number density of 4.7×10^3 cm⁻³ at the surface. The incoming flux of atomic oxygen at the Shuttle altitude is about 1.4×10^{15} atoms cm⁻²sec⁻¹, so that the production efficiency is 1.0×10^{-7} excited molecules per impacting oxygen atom. The actual efficiency could be higher because only visible photons were recorded and some fraction of the excited molecules may radiate in the infrared.

Laboratory experiments are underway to examine the surface glow. It should be noted that the magnitude of the effect depends strongly on the size of the spacecraft. In the laboratory small surfaces are exposed to the streaming oxygen atoms and detection of the glow will require a long integration time. We estimate that for a square surface 10 cm in size an exposure time approximately 30 times longer is needed to obtain the glow intensity observed on the Shuttle.

The technique presented in this paper also enables us to predict the spatial distribution of the glow for different orientations of the Shuttle and estimate the degree of contamination for proposed astronomy and aeronomy experiments to be carried on future Shuttle missions.

ACKNOWLEDGMENT

We would like to thank Dr. Tom Stevenson for helping us to use the imaging facility at CFA. This research is supported in part by the Air Force Geophysics Laboratory and in part by the Aeronomy program, Division of Atmospheric Science, National Science Foundation ATM-80-25627.

REFERENCES

1. Banks, P.M., P.R. Williamson and W.J. Raitt, Space Shuttle Glow Observations, *Geophys. Res. Lett.* **10**, 118, 1983.
2. Torr, M.R., P.B. Hays, B.C. Kennedy and J.C.G. Walker, Intercalibration of airglow observations with the Atmosphere Explorer Satellites, *Planet. Space Sci.*, **25**, 173, 1977.
3. Lee, J.H. and V.J. Abreu, Exospheric temperatures deduced from 7320-7330 Å (O⁺(⁴P)-O⁺(²D)) twilight observations, *J. Geophys. Res.*, **87**, 193, 1982.
4. Lee, J.H. and V.J. Abreu, Optical contamination on the Atmosphere Explorer-E Satellite, *Proceedings of SPIE Technical*

- Symposium, 338, 120, 1982.
5. Hays, P.B., G. Carignan, B.C. Kennedy, G.G. Shepherd and J.C.G. Walker, The Visible-Airglow Experiment on Atmosphere Explorer, *Radio Science*, 8, 369, 1973.
 6. Yee, J.H. and V.J. Abreu, Visible Glow Induced by Spacecraft-Environment interaction, *Geophys. Res. Lett.*, 10, 126, 1983.
 7. Slanger, T.G., Conjectures on the origin of the surface glow of space vehicles, *Geophys. Res. Lett.* 10, 130, 1983.
 8. Langhoff, S.R., R.L. Jaffe, J.H. Yee and A. Dalgarno, The Surface Glow of the Atmosphere Explorer C and E Satellites, in press, *Geophys. Res. Lett.*, 1983.
 9. Mende, S.B., O.K. Garriott and P.M. Banks, Observations of Optical Emissions on STS-4, *Geophys. Res. Lett.* 10, 122, 1983.
 10. Abreu, V.J., W.R. Skinner, P.B. Hays and J.H. Yee, Optical Effects of spacecraft-environment Interaction: Spectrometric Observations by the DE-B Satellite, to be presented in this conference, 1983.
 11. Mies, G.H., Calculated vibrational transition probabilities of OH ($X^2\Pi$), *J. Molec. Spectr.* 53, 150, 1974.

AIAA-83-2657

**Optical Effects of Spacecraft-Environment
Interaction: Spectrometric Observations by the
DE-B Satellite**

**V.J. ABREU, W.R. SKINNER, P.B. HAYS and
J- H. YEE**

**AIAA SHUTTLE ENVIRONMENT
AND OPERATIONS MEETING**

OCTOBER 31-NOVEMBER 2, 1983/WASHINGTON, DC

83-2657

OPTICAL EFFECTS OF SPACECRAFT-ENVIRONMENT INTERACTION:
SPECTROMETRIC OBSERVATIONS BY THE DE-B SATELLITE

Vincent J. Abreu, Wilbert R. Skinner, and Paul B. Hays
Space Physics Research Laboratory
The University of Michigan
Ann Arbor, Michigan 48109

Jeng-Hwa Yee
Harvard-Smithsonian Center for Astrophysics
Cambridge, Massachusetts 02138

Abstract

Data from the Fabry-Perot interferometer on board the Dynamics Explorer-B satellite is used to show that the contaminant glow observed by Yee and Abreu at 7320Å on the AE satellites is produced by emission lines of one or more species. A comparison is made of the contaminant spectrum near 7320Å with the nightglow OH spectrum measured below 155 km. Evidence is presented to the effect that OH might be one of the metastable species producing the glow.

I. Introduction

The characteristics and spectral variation of the optical glow induced by spacecraft-atmosphere interaction have been recently described by Yee and Abreu [1982, 1983] using photometric data obtained by the Visible Airglow Experiment (VAE) on board the Atmosphere Explorer satellites [Hays et al., 1973]. Their data showed that: 1) the most intense radiation comes from surfaces facing the direction of motion of the satellite; 2) the contamination is a band or continuum spectrum which is brighter toward the red; and 3) there is a strong correlation between emission intensity and oxygen atom density in the 160-280 km altitude range. Yee and Abreu suggested that the glow is produced by molecules which are formed and ejected from the satellite surface in a metastable state after surface particles undergo chemical reaction or direct impact collisions with incoming $O(^1P)$ atoms at the satellite velocity ($\sim 8 \text{ km sec}^{-1}$). Later, based on the apparent spectral distribution and the radiative lifetime deduced by Yee and Abreu (25 msec) Slanger [1983] showed that the OH Meinel bands are a tentative identification for the AE satellite glow. He proposed that OH is produced by the interaction of $O(^1P)$ atoms and adsorbed water and/or C-H bonds in the satellite construction material. So far, however, no spectroscopic measurements have been reported which confirm this hypothesis.

The Dynamic Explorer-B spacecraft is a modified version of the Atmosphere Explorer spacecrafts, whose payload included a high resolution Fabry-Perot interferometer (FPI) designed to measure temperature and winds in the thermosphere. Given the similarity between the spacecrafts, we have used the resolution data obtained by the FPI in a spectral region centered around 7320Å in order to provide further evidence concerning the nature of the processes producing the optical glow. The spectral region to be investigated corresponds to the OH emission band. This emission is also very strong in the terrestrial nightglow producing a narrow emission layer which peaks in the upper mesosphere. Consequently, a comparison of spectra obtained at mesospheric heights with those obtained at satellite altitudes ($\sim 250 \text{ km}$) should provide the necessary information to show whether OH is one of the emitting metastable species producing the

optical glow. This analysis is presented in this paper.

II. Description of Instrument

The Fabry-Perot interferometer on Dynamics Explorer-B is a remote sensing instrument designed mainly to measure the temperature, meridional wind and density of metastable $O(^1S)$ and $O(^1D)$ atoms and the $O^+(^2P)$ ion in the thermosphere. A detailed description of the instrument has been given by Hays et al. [1981], Killeen et al. [1983], and Killeen and Hays [1983].

The measurements are made with a high resolution Fabry-Perot etalon, which performs a wavelength analysis on light detected from atmospheric emission features by spatially scanning the interference fringe plane with 12 concentric ring detectors. The scan is linear in wavelength, covering a spectral range equal to 0.01796\AA per detector channel at 7320Å. The number of free spectral ranges focused on the detector is 1.0135 at this wavelength. The spectral region for analysis was selected by a 10Å halfwidth interference filter centered at 7320Å. The etalon and detector parameters of interest are summarized in Table 1.

Table 1 Parameters of Interferometer

1. Free Spectral range	0.21265\AA (7320Å)
2. Fraction of the free spectral range on detector	1.0135 (7320Å)
3. Detector anode structure	12 concentric rings equal area anodes
4. Spectral range per anode	0.01796\AA (7320Å)

A sequential altitude scan performed by a commandable horizon scan mirror provides the spatial information at sixteen tangent heights below the orbit of the satellite. Figure 1 is a schematic which shows the detector position relative to the velocity vector of the spacecraft, as well as the range of tangent altitudes scanned by the mirror. The altitude scan was limited to the angular region from 5 to 15 degrees below the local horizon, with a field of view of 0.9 degrees (half-cone angle).

The sensitivity of the instrument was determined in a pre-flight calibration to be .04 counts/Rayleigh-sec. For this analysis the sensitivity was also determined by an in-flight calibration using the daytime thermospheric $O^+(^2P)$ emission at 7319.079Å and 7320.154Å. The production and loss processes, as well as the reaction rates involved in the calculation of the volume emission rate of this emission are well known. The sensitivity was then estimated from a theoretical calculation of the brightness [Abreu et al., 1980] and simultaneous

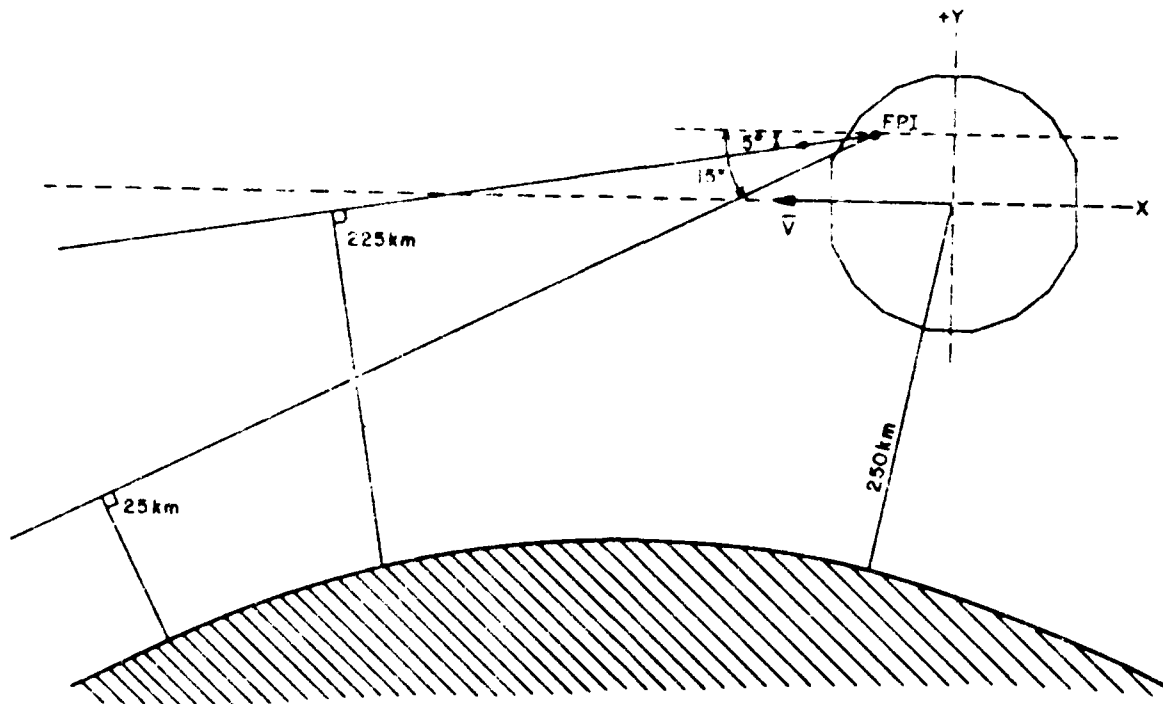


Figure 1. Schematic showing the detector position relative to the velocity vector of the spacecraft, as well as the range of tangent altitudes scanned by the mirror.

measurements of the Fabry-Perot detector counts, the thermospheric temperature and the O and N₂ densities made at the satellite altitude. Both calibrations are in good agreement.

For illustrative purposes, Figure 2 shows a spectrum of the O⁺(²P) emission at 7319.079 Å and 7319.154 Å. The units in the vertical axis are counts/integration period (I.P.). One integration period equals 0.22 sec. Since the transfer function of the Fabry-Perot is periodic, the relative position of the two lines in the image plane detector depends on $\Delta\lambda/\text{FSR}$, where $\Delta\lambda$ is the wavelength separation between the two lines and FSR is the free spectral range of the etalon. The channel separation (number of channels apart) in the image plane detector is given by

$$C_{\text{IP}} = \text{INT}(\Delta\lambda/\text{FSR}) + \text{FSR}/\Delta\lambda$$

where INT represents the integer part of the argument and $\text{INT}(\Delta\lambda/\text{FSR})$ is the integer part of the argument. The integer part of the argument is the number of channels apart, and the fractional part of the argument is the number of channels apart. The width of the line is indicated in Figure 6. The width of the line is about 1000 K.

3.1. Data Analysis

We have shown for the study spectra measured by the FPI at tangent altitudes between 225 and 250 km. The spectra were obtained during the daytime. The data were recorded in the color code. Data were recorded in the color code as follows: the tangent altitude, the date, the time, the day of the year, the day of the month, and the day of the year.

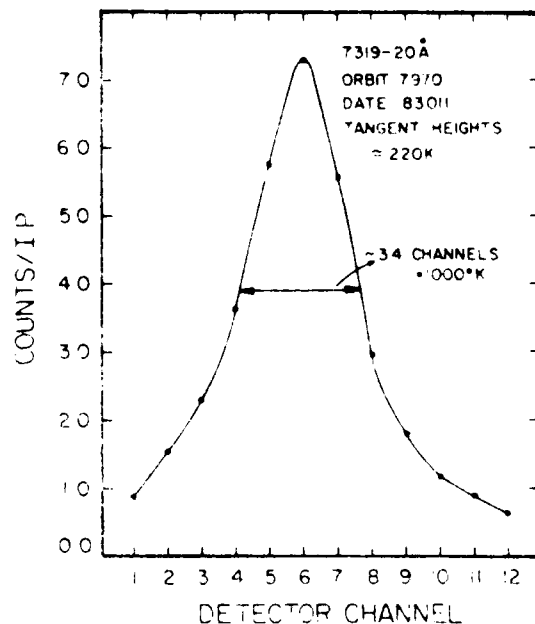
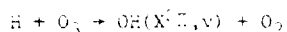


Figure 2. Spectrum of the O⁺(²P) emission obtained during the daytime.

latitude latitude was greater than 55 degrees at the satellite location. If the satellite was moving, data were rejected if the absolute value of the magnetic latitude was greater than 40 degrees at the tangent height. The above constraints insured that data were not contaminated by daytime or high latitude auroral emissions.

The most prominent feature in the spectral range of interest ($7320\text{\AA} \pm 10\text{\AA}$) in the night air-glow are the vibration-rotation transitions in the ground electronic level of OH. The excitation process for this emission is generally assigned to the reaction



(Bates and Nicolet, 1950). In general, the OH emission occurs in a thin layer which peaks around 92 km. The width of the layer is of the order of 10 km at half-intensity [Watanabe et al., 1981]. Based on the morphology of the nightglow just presented, one would expect the observed spectra below 155 km to be that of OH, while those above 155 km to be the spectra of the contaminant glow. This hypothesis will be investigated further in this analysis.

A. The Contaminant Glow Spectrum

A spectrum of the emission above 155 km has been obtained by averaging approximately 6000 nighttime spectra with tangent heights up to ~ 225 km. The average satellite altitude was 253 km. The spectrum is presented in Figure 3. The spectra had an estimated dark count removed and were normalized to remove interchannel sensitivity differences. The negative counts shown in Figure 3 are due to an imperfect knowledge of the dark count.

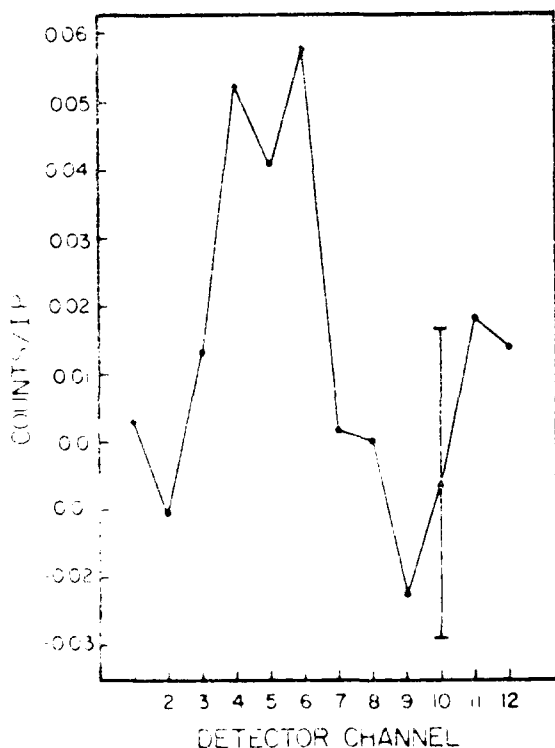


Figure 3. Spectrum of the contaminant glow.

One may wonder if the observed spectrum is that of the contaminant glow or if it is instead the spectrum of the nightglow in the thermosphere. Evidence that it is the former is provided by the fact that the same spectral shape and intensities are observed at all mirror positions with tangent heights above 155 km. Further proof is provided by comparing the photometric intensity observed here with the $7319\text{-}20\text{\AA}$ brightness of the glow observed at 250 km by Yee and Abreu [1981] using data from the VAE photometers on the Atmosphere Explorer satellites. The photometric brightness is obtained by adding the counts from each detector and multiplying the resulting counts by the calibration factor. The brightness thus obtained is ~ 20 Rayleighs. This is in good agreement with the $7319\text{-}20\text{\AA}$ contaminant emission observed at 250 km by Yee and Abreu. Consequently, we conclude that the spectrum observed above 155 km by the Fabry-Perot interferometer is that of the contaminant glow, and that the photometric brightness observed by Yee and Abreu on the AE satellites is not a continuum, but is produced by the emission lines of one or more species which remain to be identified. For this purpose we will next consider the OH spectra measured below 155 km.

B. OH Spectra

Figure 4 shows OH spectra at different tangent heights obtained during orbit 8058. The intensity of each spectrum as a function of altitude is consistent with the presence of a narrow layer which peaks at ~ 80 km. Below this altitude the spectra consists of two distinct emission lines which peak on channels 4 and 9, respectively. Above 80 km, the two lines come closer and they seem to converge at approximately 92 km. The apparent convergence of the two lines is due to a field of view effect, which comes about when the thin emission layer is viewed from above by the 12 channel detector. Under these circumstances each channel in the detector has a different field of view. The different intensities observed by the detector channels cause the distortion observed in the spectra. The distortions are greater in the outer channels of the detector. In order to correct the spectra it is necessary to effect a deconvolution for each detector channel, of the signal as a function of altitude with the field of view of the particular channel. The large uncertainties in the data, however, limit the accuracy of the inversion process and the recovered spectra are not free of distortions. We have effected the deconvolution of the spectra shown in Figure 4 and have averaged the spectra from tangent heights equal to 62, 72 and 82 km, after being normalized to their respective photometric brightness (area). The resultant spectrum is shown in Figure 5. Spectra from the topside of the emission layer were not averaged because the effect of the field of view is most significant in that region. It should be noted that the separation between the two spectral lines observed is approximately 5 channels. Laboratory measurements of the 8-3 band of OH have identified two lines at 7318.268\AA and 7318.337\AA [Coxon and Foster, 1982]. These two lines would appear 4 channels apart on the FPI detector, so there is a high probability that these are the two emission lines observed here. The absolute wavelengths of these two lines are not known to the accuracy necessary to predict their relative position to the $\text{O}^+(\text{P})$ 7320\AA line on the FPI detector.

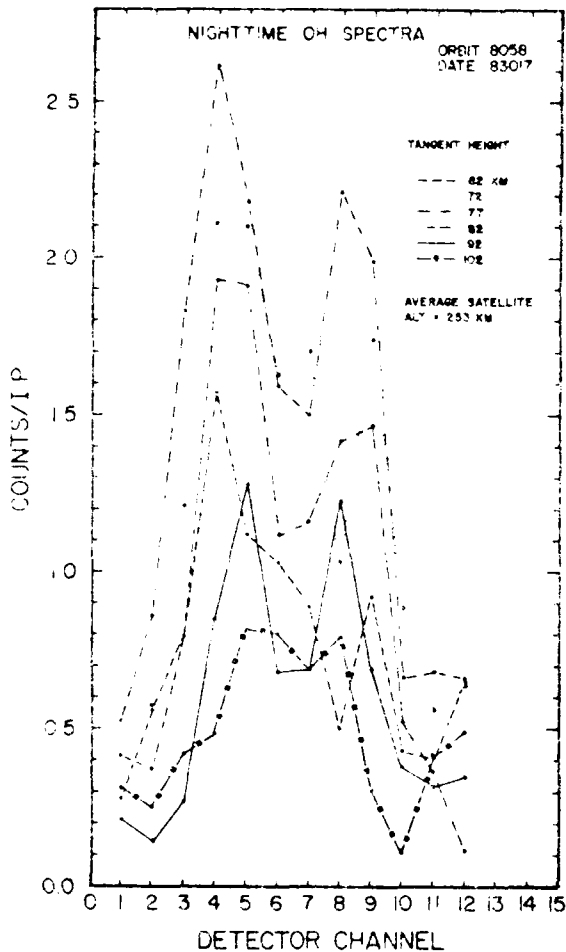


Figure 4 OH spectra at different tangent height.

The contamination spectrum, normalized to the photometric brightness is also shown in Figure 5. The shaded area indicates the statistical uncertainty in the measurements. Since the OH emission spectrum is doppler shifted by the component of the satellite velocity (~ 7.8 km/sec) along the line of sight, we have shifted the contamination spectrum by the same amount for comparison purposes.

The shape of the contaminant spectrum from channel 4 through 12 agrees well with that of the OH spectrum. This fact lends confidence to the hypothesis that OH is the contaminant species. The contaminant spectrum, however, suggests an additional peak in channel 2 which is not present on the nighttime OH spectrum. This could be another OH line or an emission line from other species. Although we have not definitively proven that OH is one of the species producing the glow, the data presented here have provided some evidence to this effect. One should be careful not to transfer these results directly to the interpretation of the glow observed in the Shuttle, since different types of contaminants are present in the shuttle environment.

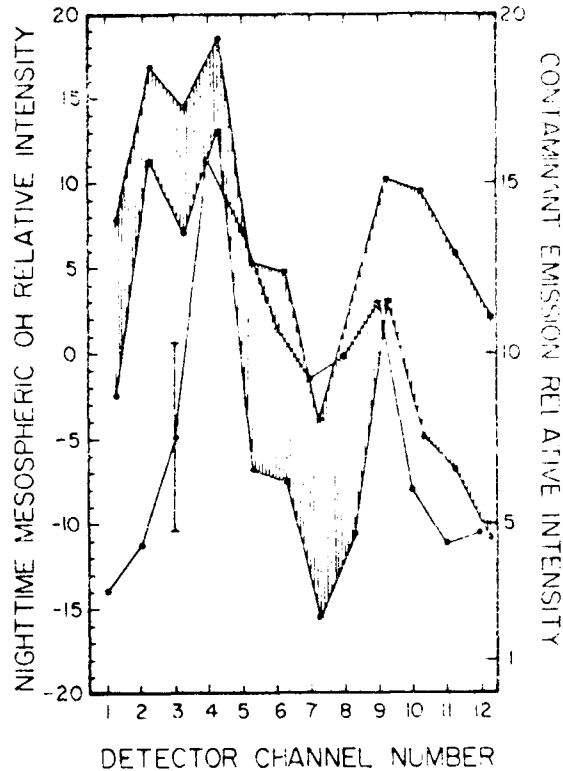


Figure 5 A comparison of the OH nightglow and the contaminant glow spectrum. The contaminant glow spectrum has been shifted by the component of the satellite velocity along the line of sight.

IV. Conclusion

Data from the Fabry-Perot interferometer on board the DE-B satellite have been used to show that the contaminant glow observed by Yee and Abreu at 7320Å on the AE satellites is produced by emission lines of one or more species. A comparison of the contaminant spectrum near 7320Å with the nightglow OH spectrum obtained below 150 km has provided evidence to the effect that OH might be one of the species producing the glow.

References

- Abreu, M.J., W.R. Skinner, and E.B. Hays, Airglow measurements of the variation of the OH(0) ionization frequency during solar cycle 21, *Geophys. Res. Lett.*, **7**, 109, 1980.
- Bates, D.R., and M. Nicolet, The photochemistry of Atmospheric water vapor, *J. Geophys. Res.*, **65**, 301, 1960.
- Coxon, J.A., and S.C. Foster, Rotational analysis of hydroxyl vibration-rotation emission bands: Molecular constants for OH X²Σ⁺, *Can. J. Phys.*, **60**, 41, 1982.

- Hays, P.B., W.B. Carlson, and B.C. Kennedy, The visible airglow experiment on Atmosphere Explorer, Space Sci. Instr., 5, 649, 1979.
- Hays, P.B., T.L. Killeen, and B.C. Kennedy, The Fabry-Perot interferometer on Dynamics Explorer, Space Sci. Instr., 5, 395, 1981.
- Killeen, T.L., B.C. Kennedy, P.B. Hays, D.A. Symonow, and D.H. Checkowski, An image plane detector for the Fabry-Perot interferometer on Dynamics Explorer, Appl. Opt., accepted for publication, August 1983.
- Killeen, T.L., and P.B. Hays, Doppler line profile analysis for a multi-channel Fabry-Perot interferometer, to be submitted to Appl. Opt., 1983.
- Sliager, T.G., Conjectures on the origin of the surface glow of space vehicles, Geophys. Res. Lett., 10, 130, 1983.
- Watanabe, T., M. Nakamura, and T. Ogawa, Rocket measurements of O_2 atmospheric and OH Meinel bands in the airglow, J. Geophys. Res., 86, 5768, 1981.
- Yee, J.H., and V.J. Abreu, Optical contamination on the Atmosphere Explorer-E satellite, Proceedings of SPIE Technical Symposium, 338, 120, 1982b.
- Yee, J.H., and V.J. Abreu, Visible glow induced by spacecraft-environment interaction, Geophys. Res. Lett., 10, 126, 1983.

Acknowledgment

This work was supported by NASA grant number NAS5-24691.

END

FILMED

7-85

DTIC